Magnetic Resonance Imaging, Fluorescence, and Drug Release Properties of Curcumin-Loaded PEGylated Magnetite@Graphene Quantum Dots Nanocomposite

Baharak Divband (PhD)[1,2,3], Amal Y. Al-Yasiri (PhD)[4], Najwan Mohammed Saeed (MSc)[4], Davood Khezerloo (PhD)[1,5], Nahideh Gharehaghaji (PhD)[1,5]*

[1]Medical Radiation Sciences Research Center, Tabriz University of Medical Sciences, Tabriz, Iran
[2]Dental and Periodontal Research Center, Tabriz University of Medical Sciences, Tabriz, Iran
[3]Inorganic Chemistry Department, Chemistry Faculty, University of Tabriz, Tabriz, Iran
[4]Department of Basic Sciences, College of Dentistry, University of Baghdad, Baghdad, Iraq
[5]Department of Radiology, Faculty of Allied Medical Sciences, Tabriz University of Medical Sciences, Tabriz, Iran

*Corresponding author: Nahideh Gharehaghaji
Department of Radiology, Faculty of Allied Medical Sciences, Tabriz University of Medical Sciences, Tabriz, Iran
E-mail: gharehaghajin@tbzmed.ac.ir

Received: 26 September 2025
Accepted: 10 November 2025

ABSTRACT

Background: Multifunctional nanosystems, containing medical imaging components and cancer therapeutic drugs, can provide early cancer diagnosis and treatment.

Objective: The aim of this study was to investigate Magnetic Resonance Imaging (MRI), anticancer drug delivery, and fluorescence properties of curcumin-loaded PEGylated magnetite@graphene quantum dots nanocomposite.

Material and Methods: In this experimental study, PEGylated magnetite@graphene quantum dots (Fe_3O_4@GQDs-PEG) nanocomposite was synthesized and loaded with curcumin (CUR-Fe_3O_4@GQDs-PEG). Then, the size, shape, magnetic property, MRI r2 relaxivity, drug loading and in vitro release, and fluorescence property of the nanocomposite were investigated. Evaluation of the cell toxicity against MCF-7 cells was performed for both unloaded and curcumin-loaded nanocomposites.

Results: The superparamagnetic nanocomposite showed high r2 relaxivity, drug release, and fluorescence property. The curcumin-loaded nanocomposite was significantly toxic to the breast cancer cell line at high concentrations.

Conclusion: CUR-Fe_3O_4@GQDs-PEG nanocomposite can be considered an anticancer drug carrier and an appropriate potential candidate for dual modal MRI and fluorescence imaging.

Citation: Divband B, Al-Yasiri AY, Mohammed Saeed N, Khezerloo D, Gharehaghaji N. Magnetic Resonance Imaging, Fluorescence, and Drug Release Properties of Curcumin-Loaded PEGylated Magnetite@Graphene Quantum Dots Nanocomposite. *J Biomed Phys Eng*. 2025;15(6):505-514. doi: 10.31661/jbpe.v0i0.2509-1994.

Keywords

Magnetite; Curcumin; Nanocomposite; Drug Release; Magnetic Resonance Imaging; Fluorescence

Introduction

Multifunctional nanoprobes can provide medical imaging and accurate targeting of tumors, leading to early cancer diagnosis and treatment [1]. Two different imaging techniques in one nanosystem lead to the advantages of both techniques [2]. For instance, in bimodal Magnetic Resonance Imaging (MRI)/fluorescence imaging, the nanosystem benefits from high spatial resolution and soft tissue contrast of MRI with good depth penetration [3], and real-time cancer pathophysiological imaging and high sensitivity cancer detection of fluorescence imaging [4].

Iron oxide nanoparticles are MRI contrast agents, which are frequently used in nanoprobes. The coating type and characteristics of the nanoparticles are important factors in their biological properties and resulted signal intensities in MRI [5]. Surface coating of the nanoparticles affects their toxicity, colloidal stability, and magnetic [6], and relaxation properties [7]. Polymer coatings are mostly used around iron oxide nanoparticles due to increasing colloidal stability in hydrophilic conditions and preventing the nanoparticles from degradation [6]. In addition to application of iron oxide nanoparticles in contrast-enhanced MRI, they have also been used as drug carriers in cancer therapy. Therefore, the nanosystems containing the nanoparticles can provide MRI-guided therapy and monitor tissue response to treatment [8]. Polymer-based nanoparticles have an effective role in drug delivery [9]. They provide controlled and tunable release of therapeutic drugs [10]. Polyethylene Glycol (PEG) is a neutral biocompatible hydrophilic polymer widely used as a coating of nanoparticles in drug delivery [11]. Iron oxide nanoparticles have also been coated with PEG for MRI application [12, 13]. PEG coating of nanoparticles is an important factor for improving their chemical and biophysical properties [11]. PEGylation of the nanocarriers decreases their uptake by the Reticuloendothelial System (RES), protein immunogenicity, and metabolic enzymes degradation. PEGylation also prolongs the blood residence of nanocarriers [14].

Curcumin is a biologically active natural polyphenol chemotherapeutic drug, which has shown inhibition of survival and proliferation of cancer cells and induces their apoptosis without side effect [15]. Besides, curcumin is a low-toxic, easily accessible, and low-cost drug for cancer treatment [16]. However, curcumin's efficiency for cancer therapy is limited due to its hydrophobicity, high metabolism rate, and short biological half-life [17]. One approach to solve the limitations is using magnetic nanoparticles as curcumin carriers [18].

Graphene Quantum Dots (GQDs) are graphene-based materials with unique properties, such as low toxicity, biocompatibility, good solubility, and excellent photoluminescence properties [19]. They have been used in the biomedical field due to their large surface-to-volume ratio, easy functionalization, and low cytotoxicity [20]. The combination of GQDs with other materials produces nanocomposites with excellent properties and high performance [21].

Accordingly, different nanostructures containing magnetic and graphene-based components and PEG were investigated for imaging and/or chemotherapeutic drug delivery. For instance, chitosan-coated iron oxide/graphene quantum dots nanohybrid was studied for MRI/fluorescence imaging and 5-fluorouracil delivery [22]. The nanocomposites containing iron oxide nanoparticles, graphene oxide, and PEG were investigated for MRI [23, 24] and doxorubicin delivery [23-25] in other studies. In addition, PEGylated iron and graphene oxide nanocomposite was investigated for curcumin delivery without focusing on MRI property [26]. Among these studies, only in one study the fluorescence property of the nanomaterial was examined [22] and it was not reported in other studies [23-26]. Based on our knowledge, a nanocomposite, containing Fe_3O_4 nanoparticles core, which was coated with PEGylated GQDs, has not been investigated for dual mode MRI and fluorescence imaging and curcumin delivery. This study aimed to investigate curcumin delivery, magnetic resonance imaging, and fluorescence property of curcumin-loaded PEGylated magnetite@graphene quantum dots nanocomposite.

Material and Methods

The study employed an in vitro experimental design, which involved the following methodological phases.

Materials

Anhydrous sodium acetate, $FeCl_3.6H_2O$, ethylenediamine/glycol, PEG 4000, and curcumin were purchased from Sigma Chemical Co.

Synthesis

Fe_3O_4 nanoparticles were prepared according to the reported method [22]. In particular, anhydrous sodium acetate (1.75 g) and $FeCl_3.6H_2O$ (1.2 g) were added to ethylenediamine/glycol and vigorously stirred at 25 °C to obtain a transparent solution. The solution was transferred into a Teflon-lined autoclave (300 mL) and heated (200 °C, 8 h). By using a magnet, the Fe_3O_4–NH_2 nanoparticles were collected, washed, and dried at 60 °C. For the preparation of Fe_3O_4–GQDs nanoparticles, a suspension of 0.5 g Fe_3O_4–NH_2 nanoparticles in distilled water was transferred to an ultrasonic bath sonicator (Sonicator 2200 MH S3; Ultrasonic Cleaner, Milano, Italy) for 10 min. Then, 20 mL suspension of the GQDs was added and transferred to the reflux setup and mechanically stirred for 48 h at 60 °C. The resulting GQDs modified Fe_3O_4 was separated by a magnet, washed, and dried under vacuum and named as Fe_3O_4@GQDs.

PEGylation of the nanocomposite was carried out by preparing a suspension of Fe_3O_4@GQDs nanoparticles in distilled water in an ultrasonic bath sonicator for 1 h, and a solution of PEG 4000 was gradually added to the suspension under continued ultrasound and heated up to 70 °C for 2 h. Then, the suspension was refluxed overnight. The as-prepared nanocomposite was washed and dried at room temperature and named Fe_3O_4@GQDs-PEG.

Characterization

The Fourier Transform Infrared (FT-IR) spectrum was recorded by a Bruker Tensor 27, using KBr pellets in the range of 400–4000 cm^{-1}. A Scanning Electron Microscope (SEM) (Tescan MIRA3 FEGSEM) was used to obtain the Fe_3O_4@GQDs nanocomposite image. Vibrating Sample Magnetometry (VSM) was performed using the VSM model 7400 to evaluate the magnetic property of curcumin-loaded Fe_3O_4@GQDs-PEG nanocomposite at room temperature. The applied magnetic fields were between -12000 and +12000 G. A monochromator-based fluorescence spectrometer (Perkin Elmer LS 55, USA) was used for the investigation of the fluorescence property of curcumin-loaded Fe_3O_4@GQDs-PEG nanocomposite. The measurements were performed at room temperature using an excitation wavelength of 360 nm and emission wavelength of 400–660 nm with pH 7.

Curcumin loading and in vitro releasing

Loading and release studies of curcumin on Fe_3O_4@GQDs-PEG nanocomposite were performed based on method reported in the previous study [27]. Typically, 1 g/10 mL suspension of the nanocomposite was mixed with curcumin solution (2 mg/mL), and stirred for 48 h at room temperature. Then, the mixture was centrifuged, washed, dried, and named CUR-Fe_3O_4@GQDs-PEG. The extent of curcumin encapsulation in the carrier was calculated considering the absorption of the supernatant by a visible spectrophotometer (Shimadzo 1700). For the investigation of in vitro release performance of the nanocomposite, 50 mg of CUR-Fe_3O_4@GQDs-PEG in 30 mL of Phosphate-Buffered Saline (PBS) was stirred at 37 °C in a dialysis bag (12 kDa). To obtain the time-dependent release profile of the curcumin, 1 mL of dialysate was taken out at the time intervals and replaced with 1 mL of the solution of fresh buffer.

MRI

The nanocomposite samples, containing 0, 0.01, 0.02, 0.03, and 0.04 mM Fe concentrations dispersed in 2% agar aqueous solution, were prepared and placed in the center of a head coil. The T2-weighted images were acquired by a 1.5 T MRI system (Magnetom Amira, Siemens, Germany) using a multi-spin echo pulse sequence. A Repetition Time (TR) of 3600 ms, Echo Time (TE) ranging between 14 and 224 ms, Number of Signal Averaging (NSA) of one, Field of View (FOV) of 192×192 mm^2, matrix size of 128×128, and slice thickness of 5 mm were used for MR imaging. The prepared images were transferred to a personal computer to measure signal intensities of the samples acquired with different TE values using Sante DICOM Viewer 3D Pro 4.9.4 software. To avoid the coil non-uniformity effect on the signal intensity of the samples, MR imaging was similarly repeated for other samples containing a constant concentration of the nanocomposite, and the correction factors were then calculated. The signal intensity of each sample with various Fe concentrations was multiplied by the related correction factor to obtain the corrected signal intensity [28]. To calculate the 1/T2 relaxation rates, the T2 curves were plotted using Matlab R2016 software using the corrected signal intensities and different TE values. The 1/T2 versus Fe concentration graph was plotted to determine the r2 relaxivity.

Cell toxicity

The cell toxicity was investigated using 3-(4, 5-dimetylthiazol- 2-yl)-2, 5-diphenyltriazolium bromide (MTT) assay based on our previous study [29]. Briefly, MCF-7 cells (Human breast cancer cell line) were cultured in 96-well plates (4×10^3 cells/well) with 200 µL media/well for 24 h at 37 °C. Different concentrations of Fe_3O_4@GQDs-PEG and CUR-Fe_3O_4@GQDs-PEG nanocomposites, including 50, 100, 200, and 400 µg/mL, were prepared and added to the culture medium for 24 h incubation. The measurement of MCF-7 cells' proliferation was done by adding 50 µL of MTT solution and 150 µL culture medium to each well. Incubation of MCF-7 cells was performed at a condition of 37 °C and 5% CO_2 for 24 h. After elimination of MTT solution, 200 µL Dimethyl Sulfoxide (DMSO) and 25 µL Sorenson buffer were added to each well, and the optical absorbance was read by an ELISA plate reader (BioTek, Bad Friedrichshall, Germany) at a wavelength of 570 nm.

Statistics

GraphPad Prism software version 10.6 was used for the data statistical analysis to determine the mean ± Standard Deviation (SD) of the results. Statistical significance was analyzed by two-way analysis of variance (ANOVA). The differences with *P*-values of $^{**}P\leq0.01$, $^{***}P\leq0.001$, and $^{****}P\leq0.0001$ were considered to be significant.

Results

Characterization results

The FT-IR spectrum of Fe_3O_4@GQDs-PEG nanocomposite is shown in Figure 1. FT-IR spectrum of the nanocomposite indicated the peaks at 480 and 559 cm^{-1} related to the Fe–O bond vibration of Fe_3O_4. The strong and broad peak of the O-H stretching (at 3440 cm^{-1}), and characteristic peak of (–CO–) of GQDs (at 1644 cm^{-1}) and (C–H) of PEG (at 2924 cm^{-1}) were appeared.

As shown in Figure 2, the morphology of the Fe_3O_4@GQDs-PEG nanocomposite is roughly spherical shape and aggregated due to its magnetic property.

The magnetization versus applied magnetic field curve for CUR-Fe_3O_4@GQDs-PEG nanocomposite is shown in Figure 3. The curve was S-shaped, and remnant magnetization, hysteresis loop, and coercivity were not seen in the curve. The saturation magnetization was 46.97.

After excitation of the CUR-Fe_3O_4@GQDs-PEG nanocomposite at 360 nm under the UV light, the emission of the nanocomposite at 442 nm revealed the fluorescence property of the nanocomposite, corresponding to the blue region of the visible light spectrum.

Curcumin loading and in vitro release

The loading of curcumin on the Fe_3O_4@

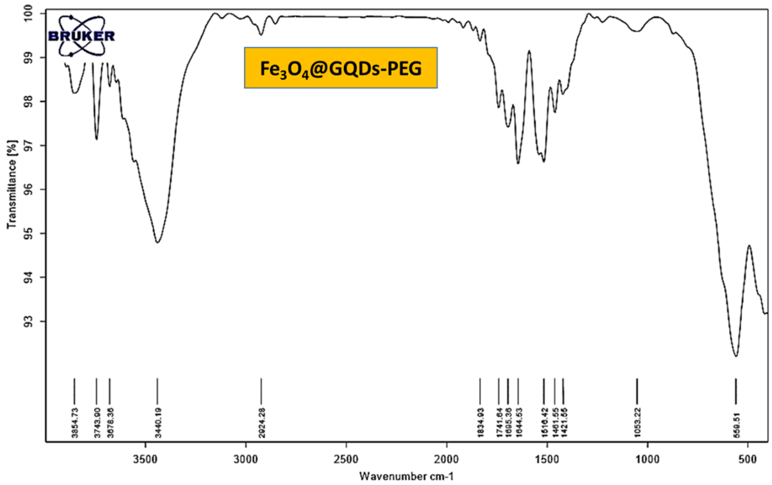

Figure 1: Fourier transform infrared spectrum of Fe_3O_4@GQDs-PEG nanocomposite

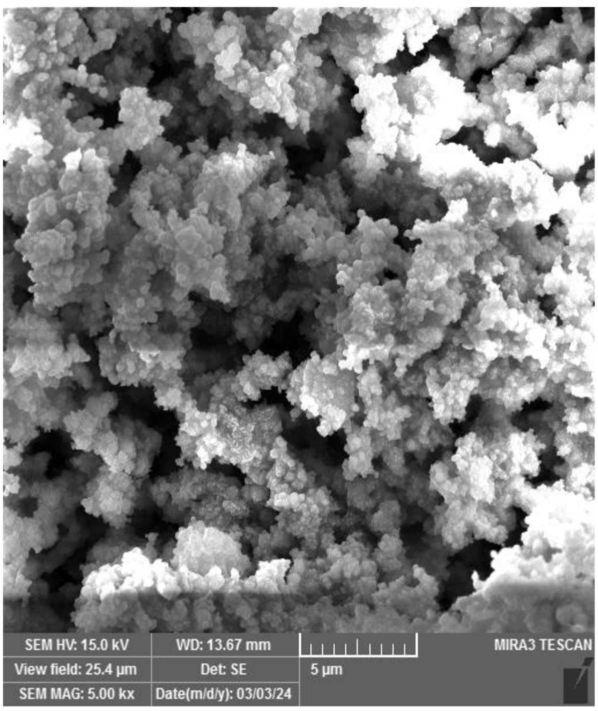

Figure 2: Scanning electron microscope image of the Fe_3O_4@GQDs-PEG nanocomposite

GQDs-PEG nanocomposite was investigated up to 10 h. The drug loading was 87% after 8 h and then reached a plateau. Loading was performed at a steep and rapid rate for the first 2 h (about 63%) and then at a gentle rate for up to 8 h.

Figure 4 illustrates the curcumin release profile from the nanocomposite during 48 h. The release percentage was about 79% after 24 h. The release was carried out with a gentle and uniform slope that continued up to 20 h. From 20-24 h, the slope became gentler, and then, it became very slow so that between 24-48 h, about 4% of the curcumin was released. Then, the release profile reached a plateau.

MRI

The T2-weighted MR image of the nanocomposite samples containing different Fe concentrations is seen in the inset of Figure 5. The signal intensity of the samples was decreased as a function of Fe concentration so that the sample containing the highest Fe concentration was seen as the darkest one. A high r2 relaxivity (786.2 $mM^{-1}S^{-1}$) was obtained based on the slope of the 1/T2 relaxation rate versus Fe concentration graph (Figure 5).

Cytotoxicity

The MTT results for Fe_3O_4@GQDs-PEG and CUR-Fe_3O_4@GQDs-PEG nanocomposites at 24 h are demonstrated in Figure 6. Both nanocomposites showed a decrease in cell viability in a concentration-dependent manner. Fe_3O_4@GQDs-PEG nanocomposite showed more than 80% cell viability up to concentrations of 200 μg/mL and nearly 80% for a

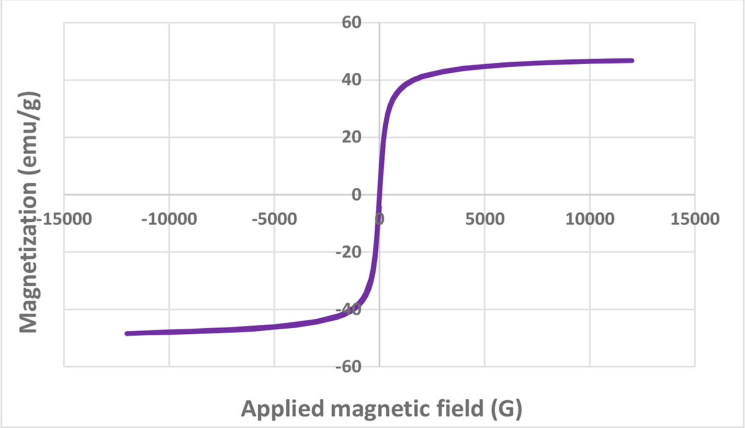

Figure 3: Magnetization curve for CUR-Fe_3O_4@GQDs-PEG nanocomposite

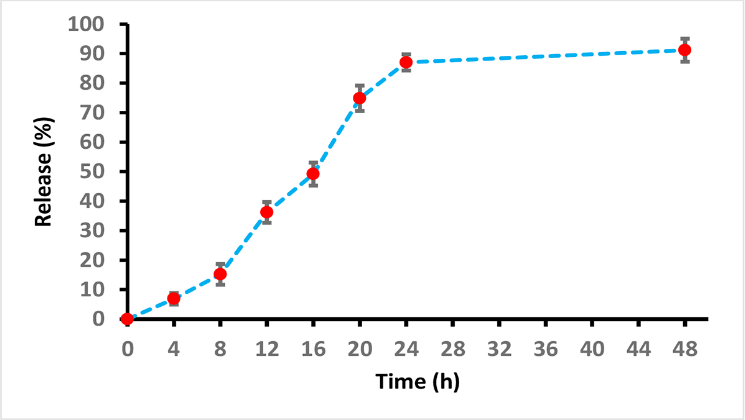

Figure 4: Release profile of curcumin from CUR-Fe_3O_4@GQDs-PEG nanocomposite

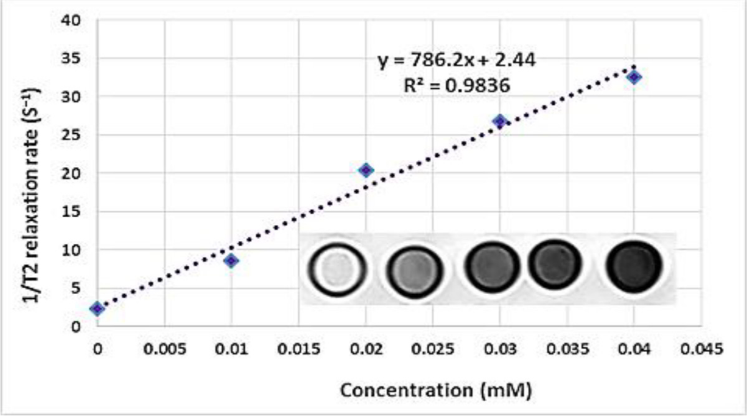

Figure 5: r2 relaxivity graph of CUR-Fe_3O_4@GQDs-PEG nanocomposite. Inset shows the T2-weighted magnetic resonance image of the nanocomposite samples containing different Fe concentrations.

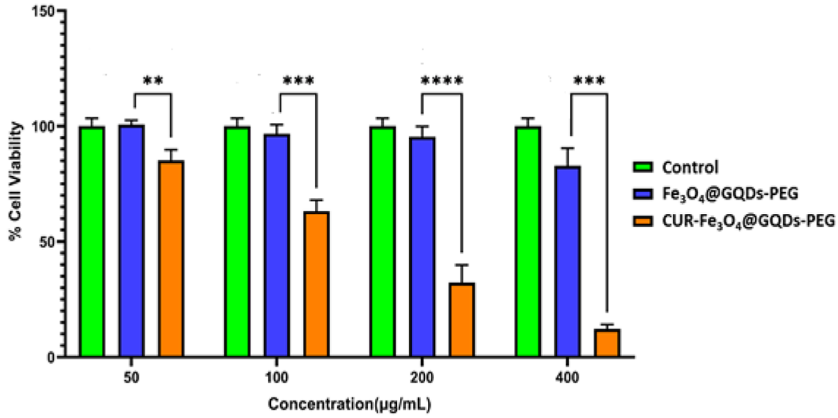

Figure 6: Cytotoxicity of Fe_3O_4@GQDs-PEG and CUR-Fe_3O_4@GQDs-PEG nanocomposites against MCF-7 cells. All data are represented as the mean ± standard deviation (n=4). Levels of $^{**}P\leq0.01$, $^{***}P\leq0.001$, and $^{****}P\leq0.0001$ were considered to be significant.

concentration of 400 µg/mL. The cell viability for CUR-Fe_3O_4@GQDs-PEG nanocomposite was higher than 80% only at a low concentration of 50 µg/mL. Then, it was dramatically decreased with the increase of CUR-Fe_3O_4@GQDs-PEG nanocomposite concentration, so that the cell viability dropped to 12% at the highest concentration of 400 µg/mL.

Discussion

Characterization tests

As reported by Pooresmaeil et al. [27], the characteristic peaks assigned to Fe_3O_4 nanoparticles and GQDs were observed in Figure 1, which revealed the successful synthesis of the Fe_3O_4@GQDs-PEG nanocomposite, showing the existence of distinctive functional groups of PEG, GQDs, and Fe_3O_4.

The SEM analysis was performed to study the morphology, size, and shape of the as-prepared nanocomposite. As shown in Figure 2, the Fe_3O_4@GQDs-PEG nanocomposite has a spherical shape, which is larger than neat GQDs and Fe_3O_4 nanoparticles [27].

Based on Figure 3, which shows the relationship between magnetization and applied magnetic field, the curve shape and absence of any remnant magnetization, hysteresis loop, and coercivity confirm the superparamagnetic property of the nanocomposite. The saturation magnetization of CUR-Fe_3O_4@GQDs-PEG was 46.97 emu/g. Compared to the results of other studies, this value is higher than the saturation magnetization of the curcumin-loaded PEGylated iron and graphene oxide (GO-Fe_3O_4-PEG-Cur) nanocomposite and close to that of GO-Fe_3O_4-PEG [26]. Despite the presence of curcumin in our nanocomposite, which reduces magnetization saturation of the nanocomposite, its value is also higher than that of PEG functionalized graphene oxide-iron oxide (GO–IONP–PEG) nanocomposite [23].

Due to the special structure of GQDs, the emission peak at 442 nm was observed, which is in agreement with other study result [27]. The fluorescence intensity for the CUR-Fe_3O_4@GQDs-PEG nanocomposite is lower than the bare GQDs and blue shifted, which could be due to aggregation of the magnetite particles. The findings of the fluorescence study demonstrated that the CUR-Fe_3O_4@GQDs-PEG nanocomposite could be considered as potential nanocomposite for future fluorescence imaging studies.

Curcumin loading and release

According to the curcumin release profile from the nanocomposite (Figure 4), the maximum drug release was observed after 24 h, which can be appropriate for both MR imaging and the drug release purposes. Despite the presence of the GQDs around the iron oxide nanoparticles, it seems they have no or little effect on the curcumin release due to their very small size and being completely surrounded by the PEG. Therefore, mainly the PEG coating is responsible for the curcumin release from the nanocomposite.

Comparing the results of this study with the curcumin release from the PEGylated Magnetite/Hydroxyapatite (PMHA) nanocomposite in our previous study [30] showed the role of both PEG and hydroxyapatite coatings in its drug release. Since hydroxyapatite has a porous structure, it can accommodate the drug and gradually release it at the target site, preventing sudden drug release. In this situation, with controlled drug release, the appropriate concentration of curcumin is maintained at the target site, which provides cancer treatment effectiveness. However, with this approach, there is not enough time for high-dose drug release. On the other hand, in the present study, PEG alone is more effective in releasing the appropriate dose of curcumin in a short period of time.

MRI

As seen in Figure 5, with increasing the Fe content of the nanocomposite samples, their darkness was increased. The presence of magnetite nanoparticles creates the local magnetic field inhomogeneities, which affect the spin-spin interactions of the surrounding water protons, leading to the shortening of the T2 relaxation time and decreasing the signal intensity of the samples based on their iron content. This signal decrease is observed as a dark region in the image. Therefore, the sample with the highest Fe concentration is the darkest one. Since the inverse T2 relaxation times (1/T2 relaxation rates) are used to plot the relaxivity graph, the samples with shorter T2s (darker samples) provide higher 1/T2 points in the graph, which can lead to obtaining a high r2 relaxivity. MRI contrast agents with high r2 relaxivity are better candidates for contrast-enhanced imaging because they can be used at lower doses, which decreases their side effects. Comparing the result of the present study with another study showed that despite loading of curcumin on Fe_3O_4@GQDs-PEG nanocomposite, its r2 relaxivity is higher than GO–IONP–PEG nanocomposite [23].

Cell toxicity

The MCF-7 cells' viability was decreased with the increase of the Fe_3O_4@GQDs-PEG nanocomposite concentration (Figure 6). However, it was higher than 80% for the concentrations up to 200 µg/mL and close to 80% for the concentration of 400 µg/mL. Therefore, the nanocomposite can be considered to be cytocompatible. On the other hand, a significant concentration-dependent cytotoxicity was seen for the cells treated with CUR-Fe_3O_4@GQDs-PEG nanocomposite. The curcumin-loaded nanocomposite was highly cytotoxic for all concentrations except for a concentration as low as 50 µg/mL, confirming its considerable toxicity for the breast cancer cells at higher concentrations. The results also showed the potential of the Fe_3O_4@GQDs-PEG nanocomposite to be used as a nanocarrier for curcumin.

Conclusion

In this study, a superparamagnetic Fe_3O_4@GQDs-PEG nanocomposite was successfully synthesized and loaded with curcumin. The release profile confirmed the nanocomposite's potential to be a nanocarrier for curcumin delivery. Besides, the nanometer size, spherical shape, superparamagnetic property, and high r2 relaxivity of CUR-Fe_3O_4@GQDs-PEG nanocomposite could make it a potential candidate for T2-weighted MRI in future in vivo studies. CUR-Fe_3O_4@GQDs-PEG nanocomposite also showed fluorescence property, which suggests its potential application for future fluorescence imaging studies.

Authors' Contribution

B. Divband: Design of the study, Methodology, Investigation, Formal analysis, Data curation, Conceptualization, Resources. AY. Al-Yasiri: Data analysis and Methodology. N. Mohammed Saeed: Data analysis. D. Khezerloo: Investigation, Formal analysis. N. Gharehaghaji: Project administration, Methodology, Resources, Validation, and Funding acquisition. All authors contributed to the design of the study, and they wrote and reviewed the manuscript.

Ethical Approval

This study was approved by the Research Ethics Committees of the Vice Chancellor in Research Affairs - Tabriz University of Medical Sciences (Ethical code: IR.TBZMED.VCR.REC.1401.104).

Funding

This study was financially supported by the Faculty of Allied Medical Sciences of Tabriz University of Medical Sciences (Grant No: 70089).

Conflict of Interest

None

References

1. Xuan Y, Gao Y, Guan M, Zhang S. Application of "smart" multifunctional nanoprobes in tumor diagnosis and treatment. *J Mater Chem B.* 2022;**10**(19):3601-13. doi: 10.1039/d2tb00326k. PubMed PMID: 35437560.
2. Gharehaghaji N, Divband B, Bakhtiari-Asl F. Utilization of innovative hydroxyapatite-coated Gd2O3@ Bi2O3 nanocomposite as a bifunctional material for magnetic resonance imaging and computed tomography. *Bionanoscience.* 2020;**10**(4):909-16. doi: 10.1007/s12668-020-00787-1.
3. Mastrogiacomo S, Dou W, Jansen JA, Walboomers XF. Magnetic Resonance Imaging of Hard Tissues and Hard Tissue Engineered Bio-substitutes. *Mol Imaging Biol.* 2019;**21**(6):1003-1019. doi: 10.1007/s11307-019-01345-2. PubMed PMID: 30989438.
4. Liu L, Liu L, Pan Y, Wang S, He Y, Gong D, Zha Z. Multifunctional nanoprobes for the cancer cells pathophysiological processes sensing and imaging. *Appl Mater Today*. 2024;**36**:102028. doi: 10.1016/j.apmt.2023.102028.
5. Oghabian MA, Guiti M, Haddad P, Gharehaghaji N, Saber R, Alam NR, et al. Detection sensitivity of MRI using ultra-small super paramagnetic iron oxide nano-particles (USPIO) in biological tissues. *Conf Proc IEEE Eng Med Biol Soc*. 2006;**2006**:5625-6. doi: 10.1109/IEMBS.2006.260131. PubMed PMID: 17945909.
6. Barrow M, Taylor A, Murray P, Rosseinsky MJ, Adams DJ. Design considerations for the synthesis of polymer coated iron oxide nanoparticles for stem cell labelling and tracking using MRI. *Chem Soc Rev*. 2015;**44**(19):6733-48. doi: 10.1039/c5cs00331h. PubMed PMID: 26169237.
7. Arosio P, Orsini F, Brero F, Mariani M, Innocenti C, Sangregorio C, Lascialfari A. The effect of size, shape, coating and functionalization on nuclear relaxation properties in iron oxide core-shell nanoparticles: a brief review of the situation. *Dalton Trans*. 2023;**52**(12):3551-62. doi: 10.1039/d2dt03387a. PubMed PMID: 36880505.
8. Rahman M. Magnetic Resonance Imaging and Iron-oxide Nanoparticles in the era of Personalized Medicine. *Nanotheranostics*. 2023;**7**(4):424-49. doi: 10.7150/ntno.86467. PubMed PMID: 37650011. PubMed PMCID: PMC10464520.
9. Kateb B, Chiu K, Black KL, Yamamoto V, Khalsa B, Ljubimova JY, et al. Nanoplatforms for constructing new approaches to cancer treatment, imaging, and drug delivery: what should be the policy? *Neuroimage.* 2011;**54**(Suppl 1):S106-24. doi: 10.1016/j.neuroimage.2010.01.105. PubMed PMID: 20149882. PubMed PMCID: PMC3524337.
10. Liechty WB, Kryscio DR, Slaughter BV, Peppas NA. Polymers for drug delivery systems. *Annu Rev Chem Biomol Eng*. 2010;**1**:149-73. doi: 10.1146/annurev-chembioeng-073009-100847. PubMed PMID: 22432577. PubMed PMCID: PMC3438887.
11. Shi L, Zhang J, Zhao M, Tang S, Cheng X, Zhang W, et al. Effects of polyethylene glycol on the surface of nanoparticles for targeted drug delivery. *Nanoscale.* 2021;**13**(24):10748-64. doi: 10.1039/d1nr02065j. PubMed PMID: 34132312.
12. Meisel CL, Bainbridge P, Mulkern RV, Mitsouras D, Wong JY. Assessment of Superparamagnetic Iron Oxide Nanoparticle Poly(Ethylene Glycol) Coatings on Magnetic Resonance Relaxation for Early Disease Detection. *IEEE Open J Eng Med Biol.* 2020;**1**:116-

22. doi: 10.1109/OJEMB.2020.2989468. PubMed PMID: 33294851. PubMed PMCID: PMC7720857.

13. Ge J, Li C, Wang N, Zhang R, Afshari MJ, Chen C, et al. Effects of PEG Chain Length on Relaxometric Properties of Iron Oxide Nanoparticles-Based MRI Contrast Agent. *Nanomaterials (Basel)*. 2022;**12**(15):2673. doi: 10.3390/nano12152673. PubMed PMID: 35957104. PubMed PMCID: PMC9370369.

14. Kolate A, Baradia D, Patil S, Vhora I, Kore G, Misra A. PEG - a versatile conjugating ligand for drugs and drug delivery systems. *J Control Release.* 2014;**192**:67-81. doi: 10.1016/j.jconrel.2014.06.046. PubMed PMID: 24997275.

15. Salem M, Rohani S, Gillies ER. Curcumin, a promising anti-cancer therapeutic: a review of its chemical properties, bioactivity and approaches to cancer cell delivery. *RSC Adv.* 2014;**4**(21):10815-29. doi: 10.1039/c3ra46396f.

16. Yallapu MM, Jaggi M, Chauhan SC. Curcumin nanomedicine: a road to cancer therapeutics. *Curr Pharm Des.* 2013;**19**(11):1994-2010. doi: 10.2174/138161213805289219. PubMed PMID: 23116309. PubMed PMCID: PMC3640558.

17. Pourmadadi M, Abbasi P, Eshaghi MM, Bakhshi A, Manicum AL, Rahdar A, et al. Curcumin delivery and co-delivery based on nanomaterials as an effective approach for cancer therapy. *J Drug Deliv Sci Technol.* 2022;**78**:103982. doi: 10.1016/j.jddst.2022.103982.

18. Moballegh Nasery M, Abadi B, Poormoghadam D, Zarrabi A, Keyhanvar P, Khanbabaei H, et al. Curcumin Delivery Mediated by Bio-Based Nanoparticles: A Review. *Molecules.* 2020;**25**(3):689. doi: 10.3390/molecules25030689. PubMed PMID: 32041140. PubMed PMCID: PMC7037405.

19. Balkanloo PG, Sharifi KM, Marjani AP. Graphene quantum dots: Synthesis, characterization, and application in wastewater treatment: A review. *Mater Adv.* 2023;**4**(19):4272-93. doi: 10.1039/D3MA00372H.

20. Barati F, Avatefi M, Moghadam NB, Asghari S, Ekrami E, Mahmoudifard M. A review of graphene quantum dots and their potential biomedical applications. *J Biomater Appl.* 2023;**37**(7):1137-58. doi: 10.1177/08853282221125311. PubMed PMID: 36066191.

21. Facure MH, Schneider R, Mercante LA, Correa DS. A review on graphene quantum dots and their nanocomposites: from laboratory synthesis towards agricultural and environmental applications. *Environ Sci Nano.* 2020;**7**(12):3710-34. doi: 10.1039/D0EN00787K.

22. Hassani S, Gharehaghaji N, Divband B. Chitosan-coated iron oxide/graphene quantum dots as a potential multifunctional nanohybrid for bimodal magnetic resonance/fluorescence imaging and 5-fluorouracil delivery. *Mater Today Commun*. 2022;**31**:103589. doi: 10.1016/j.mtcomm.2022.103589.

23. Ma X, Tao H, Yang K, Feng L, Cheng L, Shi X, et al. A functionalized graphene oxide-iron oxide nanocomposite for magnetically targeted drug delivery, photothermal therapy, and magnetic resonance imaging. *Nano Res.* 2012;**5**(3):199-212. doi: 10.1007/s12274-012-0200-y.

24. Chen W, Wen X, Zhen G, Zheng X. Assembly of Fe 3 O 4 nanoparticles on PEG-functionalized graphene oxide for efficient magnetic imaging and drug delivery. *RSC Adv*. 2015;5(85):69307-11. doi: 10.1039/C5RA09901C.

25. Ramezani Farani M, Khadiv-Parsi P, Riazi GH, Shafiee Ardestani M, Saligheh Rad H. PEGylation of graphene/iron oxide nanocomposite: assessment of release of doxorubicin, magnetically targeted drug delivery and photothermal therapy. *Appl Nanosci.* 2020;**10**(4):1205-17. doi: 10.1007/s13204-020-01255-8.

26. Abbasi R, Mostafavi Amjad J, Nosrati H, Mohammadkhani R, Danafar H. Synthesis and characterization of PEGylated iron and graphene oxide magnetic composite for curcumin delivery. *Appl Organomet Chem*. 2020;**34**(10):e5825. doi: 10.1002/aoc.5825.

27. Pooresmaeil M, Namazi H. pH-sensitive ternary Fe3O4/GQDs@ G hybrid microspheres; Synthesis, characterization and drug delivery application. *J Alloys Compd*. 2020;**846**:156419. doi: 10.1016/j.jallcom.2020.156419.

28. Nazarpoor M. Non-uniformity of clinical head, head and neck, and body coils in Magnetic Resonance Imaging (MRI). *Iran J Med Phys.* 2014;**11**(4):322-7. doi: 10.22038/ijmp.2014.3569.

29. Gharehaghaji N, Divband B, Zareei L. Nanoparticulate NaA zeolite composites for MRI: Effect of iron oxide content on image contrast. *J Magn Magn Mater.* 2018;**456**:136-41. doi: 10.1016/j.jmmm.2018.02.013.

30. Gharehaghaji N, Divband B. PEGylated Magnetite/Hydroxyapatite: A Green Nanocomposite for T2-Weighted MRI and Curcumin Carrying. *Evid Based Complement Alternat Med.* 2022;**2022**:1337588. doi: 10.1155/2022/1337588. PubMed PMID: 35722138. PubMed PMCID: PMC9201731.